

MODULATION AND CODING FOR FAST FADING MOBILE SATELLITE COMMUNICATION CHANNELS

P.J. MCLANE, P.H. WITKE, W.S. SMITH, A. LEE, Department of Electrical Engineering, Queen's University, Canada; P.K.M. HO, Simon Fraser University, Canada; C. LOO, Department of Communications, Canada.

DEPARTMENT OF ELECTRICAL ENGINEERING
Queen's University
Kingston, Ontario
K7L 3N6
Canada

ABSTRACT

The first part of this paper describes the performance of GMSK using differential detection in fast Rician fading, with a novel treatment of the inherent ISI leading to an exact solution. In the second part trellis coded DPSK with a convolutional interleaver is considered. The channel is the Rician Channel with the line-of-sight component subject to a lognormal transformation. This accounts for shadowing on the Rician Channel.

INTRODUCTION

We consider digital transmission using phase modulation over the Rician Channel. This is meant to model a mobile satellite communications link. In the first part of the paper, which is based on [Smith, 1988], GMSK is considered from an analytical point of view for the Rician case. In the second part we treat shadowing and trellis coded DPSK via Monte Carlo simulation.

GMSK IN FAST RICIAN FADING

The problem addressed here is that of obtaining an explicit analytical expression for the error performance of Gaussian baseband filtered minimum shift keying, (GMSK), using differential detection in a fast Rician fading channel with additive Gaussian noise [Smith, 1988]. This problem can be divided into two sections, namely determining the probability of error conditioned on a specific phase change over the bit period, and accounting for the intersymbol interference (ISI) inherent in GMSK modulation. The solution to the first has been reported in [Mason, 1987]. He points out that an alternate treatment is given in [Stein, 1964], which will be the approach taken here. The second step is accomplished by a new technique which allows the calculation of the expected value of a function over the probability distribution of the interference

variables. This method results in an exact explicit expression for the error probability which may be calculated to the desired degree of accuracy. The procedure is generally applicable in a wide range of digital communications problems involving ISI.

A GMSK signal is generated by passing a non-return-to-zero data stream through a Gaussian baseband filter followed by an FM modulator with modulation index 0.5. The transmitted GMSK data phase signal may be represented as

$$\theta(t) = \pi \int_{-\infty}^t \sum_{n=-\infty}^{\infty} a_n \left(\frac{1}{2T}\right) g(v - nT) dv \quad (1)$$

where $\{a_n\}_{n=-\infty}^{\infty}$ is a sequence of independent, identically distributed random variables taking on the values +1 or -1 with equal probability, T is the bit period, and g(t), the basic frequency pulse, is given in [Simon and Wang, 1984, eqn. 18]. The factor (1/2T) normalizes g(t) such that the net phase change due to one data bit, after FM modulation with index 0.5, is $\pi/2$.

The receiver consists of a standard differential detector, where the predetection bandpass filter and postdetection baseband filter are assumed to have negligible effect on the signal components. Considering a lowpass equivalent representation, the received signal at the input to the differential detector, z(t), consists of the direct component $u(t) = A \exp[j\theta(t)]$, the Rayleigh faded component $r(t) = w(t)\exp[j\theta(t)]$, and the additive Gaussian noise n(t), where A is the signal amplitude, and w(t) and n(t) are mutually independent stationary zero-mean complex Gaussian processes. The differential detector acts as a quadrature product demodulator forming the output $v(t) = (1/2)\text{Re}\{-jz(t)z^*(t - T)\}$ where * denotes conjugation, $\text{Re}\{\cdot\}$ denotes the real part of $\{\cdot\}$, and it is assumed that the carrier radian frequency $\omega = n2\pi/T$ for n an integer. This is sampled at times $t = T/2 + nT$ and the data is recovered based on the polarity of $v(T/2 + nT)$.

Consider the detection of the zeroth bit, assumed +1. Conditioned on receiving a particular phase change, $\Delta\theta = \theta(T/2) - \theta(-T/2)$, $z(T/2)$ and $z(-T/2)$ are dependent conditional complex Gaussian variables. Following the development given in [Stein, 1964], the probability of error may be expressed as

$$P(\text{error} | \Delta\theta, a_0 = 1) = 1/2 [1 - Q(\sqrt{b}, \sqrt{a}) + Q(\sqrt{a}, \sqrt{b})] - \frac{C}{2} \exp\left(-\frac{(a+b)}{2}\right) I_0(\sqrt{ab}) \quad (2)$$

$$\text{where } \begin{Bmatrix} a \\ b \end{Bmatrix} = \frac{KA}{D} [(\Lambda + K + 1) - \Lambda \rho_s \cos^2 \Delta\theta - (K + 1) \rho_n \cos \Delta\theta \mp \sqrt{D} \sin \Delta\theta]$$

$$C = (\Lambda \rho_s \sin \Delta\theta) / \sqrt{D} \quad D = (\Lambda + K + 1)^2 - (\Lambda \rho_s \cos \Delta\theta + \rho_n (K + 1))^2$$

where $\rho_s = J_0(2\pi f_D T)$, is the normalized autocorrelation function for the mobile fading spectrum with maximum Doppler frequency f_D , $\rho_n = \sin(2\pi B_{IF} T) / (2\pi B_{IF} T)$ is the normalized autocorrelation of the noise for an ideal rectangular bandpass filter with one-sided bandwidth B_{IF} ,

K is the propagation SNR, Λ is the average SNR, $Q(\alpha, \beta)$ is Marcum's Q-function and I_0 and J_0 are Bessel functions.

The foregoing analysis is conditioned on the value of the phase change over the bit interval, which depends on the infinite sequence of data bits being transmitted.

$$\begin{aligned} \Delta\theta &= \pi \sum_{k=-\infty}^{\infty} a_k \int_{-T/2}^{T/2} \left(\frac{1}{2T}\right) g(v-kT) dv \\ &= a_0 \beta_0 + \sum_{k=1}^{\infty} a_{-k} \beta_k + \sum_{k=1}^{\infty} a_k \beta_k = \beta_0 + X + Y \end{aligned} \quad (3)$$

$$\text{where } \beta_k = \beta_{-k} = \pi \int_{-T/2}^{T/2} \left(\frac{1}{2T}\right) g(v-kT) dv$$

$$X = \sum_{k=1}^{\infty} a_{-k} \beta_k \quad Y = \sum_{k=1}^{\infty} a_k \beta_k$$

In (3), a_0 the data bit being detected is assumed to be +1, and X and Y are independent random variables with identical distributions. It can be shown that the variables X and Y are singular and of the Cantor type, [Wittke et al., 1988], provided that $BT > 0.0784$. In this case, the probability distribution function of X or Y is a continuous function that takes on constant values except on a set of measure zero. The expected value of a general function conditioned on one interference variable, say X, may be evaluated as

$$E\{f(X)\} = f(R_1) - \sum_{j=1}^{\infty} \sum_{k=1}^{2^{j-1}} (2k-1) 2^{-j} [f(E_{jk}) - f(S_{jk})] \quad (4)$$

$$\text{where } S_{jk} = \gamma_{j-1, k}^{-\rho_j}, \quad E_{jk} = \gamma_{j-1, k}^{+\rho_j}, \quad \rho_j = \beta_j^{-R_{j+1}}, \quad R_j = \sum_{k=j}^{\infty} \beta_k,$$

$\gamma_{j,k}$ can take on the 2^j values, $\pm \beta_1, \pm \beta_2, \dots, \pm \beta_j$ and are ordered in increasing value, and γ_{01} has been defined as zero. Conditioning on two independent identically distributed Cantor variables, as is required by this analysis, leads to the result

$$\begin{aligned} E\{f(X, Y)\} &= f(R_1, R_1) + \sum_{j=1}^{\infty} \sum_{k=1}^{2^{j-1}} \sum_{m=1}^{\infty} \sum_{n=1}^{2^{m-1}} (2k-1) 2^{-j} (2n-1) 2^{-m} \\ &\cdot [f(S_{mn}, S_{jk}) + f(E_{mn}, E_{jk}) - f(S_{mn}, E_{jk}) - f(E_{mn}, S_{jk})] + \end{aligned}$$

$$\sum_{j=1}^{\infty} \sum_{k=1}^{2^{j-1}} (2k-1) 2^{-j} [f(R_1, S_{jk}) + f(S_{jk}, R_1) - f(R_1, E_{jk}) - f(E_{jk}, R_1)] \quad (5)$$

Combining the previous two results, equations (2) and (5) gives the overall error probability. This has been plotted in Fig. 1 for varying premodulation bandwidth BT , with propagation SNR $K = 10$ dB, maximum Doppler frequency $f_D T = 0.05$, and one-sided 3 dB bandpass filter bandwidth $B_{IF} T = 1.0$. These parameters are typical of the conditions expected for the Canadian MSAT program. In evaluating the error probability, the number of terms required for 3 figure accuracy decreases with increasing premodulation filter bandwidth, BT . For example the curve for $BT=0.3$ was evaluated by truncating the series beyond $j=m=2$, and for $BT=0.5$ beyond $j=m=1$.

TCM WITH D8PSK

In this section we report on the use of interleaved, trellis coded modulation used in conjunction with D8PSK modulation. A block diagram of the system under consideration is shown in Fig. 2. Here the burst error channel is modelled as an additive white Gaussian noise channel where the gain and phase are modeled as a random process. This dynamically varying phasor represents non-static signal fading.

Most investigations [Simon and Divsalar, 1986] use the Rician model for signal fading which is composed of a constant line-of-sight (LOS) component plus a scatter component which is a complex Gaussian random process. In Canada, due to a low angle of elevation to the satellite, a shadowed Rician model has been developed [Loo, 1985]. This model has the same scatter component as the Rician, but the LOS component is subjected to a lognormal transformation. The dynamics of the fading is controlled by a third-order-Butterworth filter.

System performance is determined by digital computer simulation of the fading channel. A single sample per symbol interval is used to represent the fading process. Results using this model for 4- and 8-state trellis coded PSK and DPSK modulations were reported in [McLane et al., 1987]. It was found that for up to average shadowing conditions a fade margin of 12 dB could be maintained at a BER of 10^{-3} ; this is a relevant BER as speech transmission is regarded as the major application.

In [McLane et al., 1987] interleaved transmission was treated only from an approximate point of view. We have included the convolutional interleaver shown in Fig. 3 into our simulations. Such a convolutional interleaver is ideal for use with Ungerboeck codes as such codes use convolutional encoders as generators. Also, convolutional interleavers have lower delay than block interleavers. This is important in speech applications where the overall delay must be kept below 300 ms. As the propagation delay in MSAT is 250 ms this leaves 50 ms for Viterbi decoder plus convolutional interleaver delay. The results of our simulations are shown in Fig. 4. The case $\lambda = 6$

meets the 50 msec constraint but the $\lambda = 8$ case does not. However, we have recently found, as suggested in [McLane et al., 1987], that the Viterbi decoding delay can be reduced to make $\lambda = 8$ meet the 50 msec time delay constraint and with very little loss in BER.

CONCLUSION

Analytical techniques to determine the performance of GMSK in a fast fading Rician Channel have been presented. For TCM and DPSK modulation, system simulation has been used to determine performance when convolutional interleavers are used. We are currently applying our analytical techniques to the TCM case.

REFERENCES

- Divsalar, D. and M.K. Simon. 1986. Trellis coded modulation for 4800 to 9600 bps transmission over a fading satellite channel. JPL Publication 86-8. (Pasadena, California): also, IEEE Journal Selected Areas Comm., Vol. SAC-5, pp. 162-175, Feb. 1987.
- Loo, C. 1985. A statistical model for a land mobile satellite link. IEEE Trans. Vehicular Technology, Vol. VT-34, pp. 122-127.
- Mason, L.J. 1987. Error probability evaluation for systems employing differential detection in a Rician fast fading environment and Gaussian noise. IEEE Trans. Commun., Vol. COM-35, pp. 39-46.
- McLane, P.J., P.H. Wittke, P.K.-M. Ho and C. Loo. 1987. Performance of binary multi-h modulation for fast fading, shadowed, mobile satellite communications. IEEE Vehicular Technology Conference. (Tampa, Florida).
- Simon, M.K. and C.C. Wang. 1984. Differential detection of Gaussian MSK in a mobile radio environment. IEEE Trans. Veh. Technol., Vol. VT-33, pp. 307-320.
- Smith, W.S. 1988. Ph.D. dissertation, Queen's University, Canada.
- Stein, S. 1964. Unified analysis of certain coherent and noncoherent binary communication systems. IEEE Trans. Inform. Theory, Vol. IT-10, pp. 43-51.
- Wittke, P.H., W.S. Smith and L.L. Campbell. Infinite series of interference variables with Cantor-type distributions. Submitted to IEEE Trans. Inform. Theory.

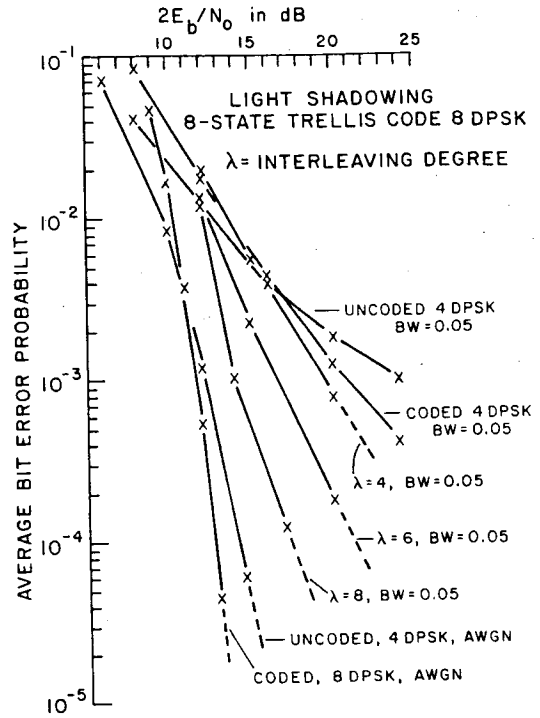
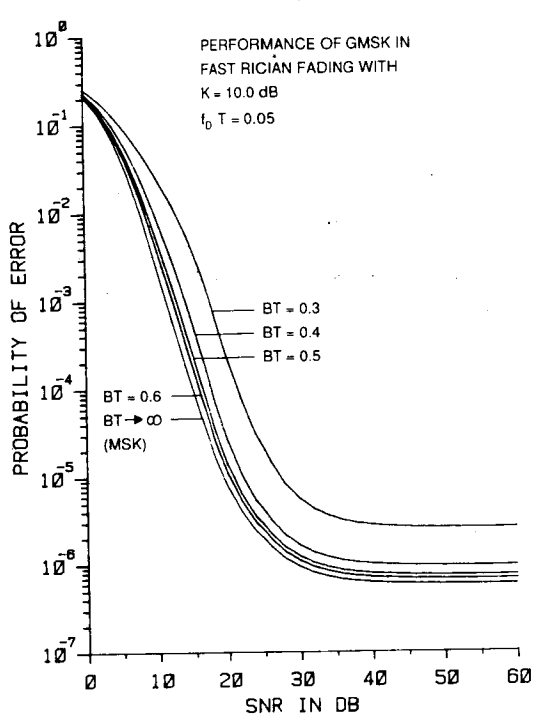


Fig. 1: GMSK Performance Fig. 4: Coded DPSK Performance

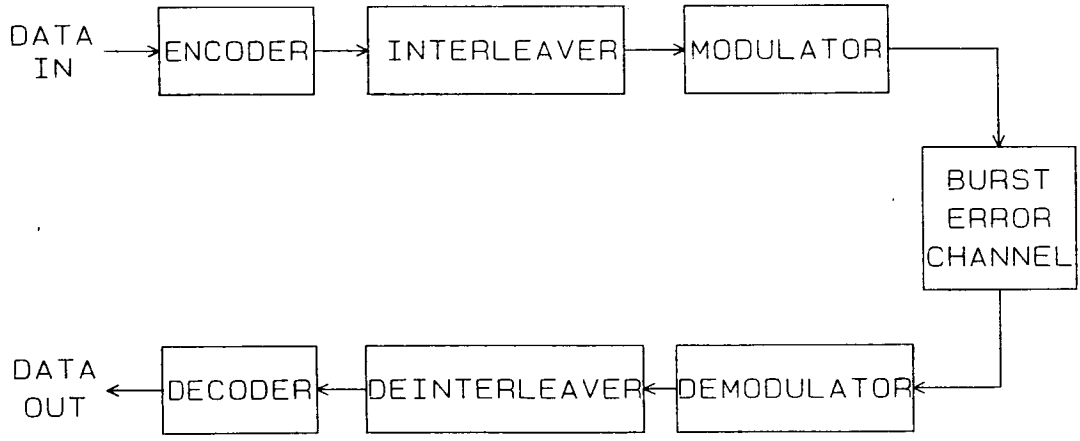


Fig. 2: Block Diagram, Interleaved and Coded DPSK

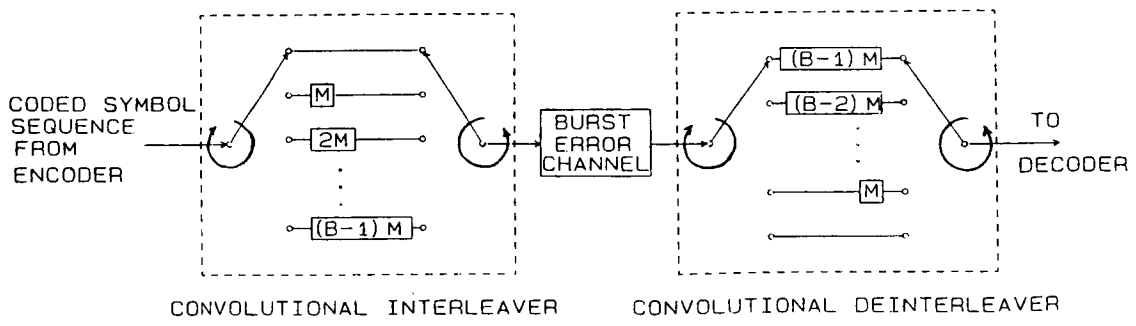


Fig. 3: Convolutional Interleaver for DPSK Trellis Codes